UDC 681.518

O. A. Sushchenko, Dr. of Sc. (National Aviation University, Ukraine)
N. D. Novytska (National Aviation University, Ukraine)
Y. M. Bezkorovainyi, Cand.of Sc. (National Aviation University, Ukraine)
V. O. Golitsyn (National Aviation University, Ukraine)

Robust control of system with nonorthogonal MEMS arrays

The paper deals with synthesis of robust system assigned for operation on unmanned aerial vehicles. A feature of the system lies in using nonorthoginal arrays of gyroscopes designed on microelectromechanical technologies. Synthesis of the controller was carried out by means of the robust structural synthesisis. Analysis of the possibility to use nonorthogonal arrays of inertial sensores was given. Results of synthesied system simulation are represented. The obtained results can be useful for moving vehicles of the wide class.

Introduction and problem statement

Nowadays using of robust control is one of the modern trends in design of complex systems. It is known also that accuracy and reliability of navigation information is of great importance for successful functioning of the complex control system in difficult conditions of real operation. Obtaining of navigation information for complex control systems operating on the board of moving vehicles can be implemented by means of accelerometers and gyroscopes manufactured on technologies of micro-electro-mechanical systems (MEMS). Such an approach ensures low cost, small sized and low power consumption of complex control systems. To improve accuracy of navigation information is possible using structural redundancy of primary navigation measuring instruments based on nonorthogonal MEMS arrays [1]. The proposed approach can be considered on the basis of the robust system with redundant nonorthogonal measuring system assigned for operation on unmanned aerial vehicles (UAVs).

There are two the most widespread approaches to implementation of structural redundancy of navigation measuring instruments. The first approach lies in using redundant inertial measuring instruments. In this case it is necessary to use the highly productive computing unit that complicates architecture and increases the price of the control system as a whole. The second approach is using of redundant sensors as components of the single measuring instrument. In this case requirements to computational burden and capacity of data transmission channel are greatly less in comparison with the first approach. So, the second approach to using of structural redundancy seems more preferable [2].

There are some configurations of nonorthogonal redundant measuring instruments based on MEMS arrays of inertial sensors [3]. Choice of configuration is defined by the concrete requirements to the control system operated on UAV.

The generalised structural scheme of UAV navigation system using redundant measuring instruments is given in Fig. 1.

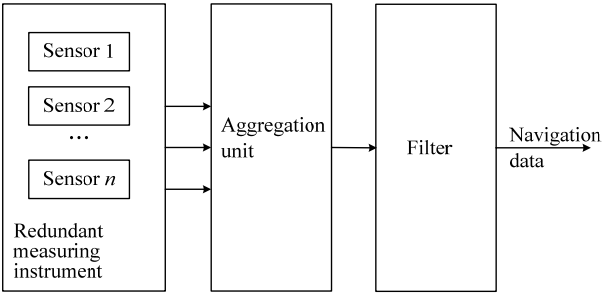

Fig. 1. The structural scheme of the redundant inertial measuring system

Respectively, the structural scheme of the system of UAV motion control can be represented by the scheme shown in Fig. 2.

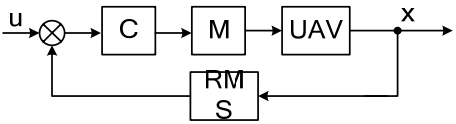

Fig. 2. The structural scheme of the system, which controls UAV motion: C is the controller; M is the motor;
RMS is redundant measuring instrument

The problem statement foresees solving some interrelated tasks. The first task is choice of nonorthogonal redundant configuration and aggregation algorithm. The main goal of the aggregation algorithm is transformation of data entering from MEMS arrays of inertial sensors into projections of the navigation parameters (accelerations, angular rates) onto the axes of the navigation reference frame. The second task is design of the robust controller based on the H_∞-synthesis.

Choice of nonorthogonal configuration of inertial sensors

Different types of nonorthogonal configurations based on MEMS arrays of inertial sensors (gyroscopes) are represented in [3]. To simplify process of robust system design it is convenient to consider nonorthogonal configuration based on single (uniaxial) sensors. It is known that one of the most widespread nonortogonal configurations is based on such geometrical figure as a cone [4]. In this case sensitivity axes of sensors are oriented along a cone's generatrices.

The results of the comparative analysis of accuracy for different nonorthogonal configurations of uniaxial sensors are represented in Table 1 [5]. This table includes data about values of traces of the correlation matrices of errors for various nonorthogonal redundant configurations in different situations of sensor failures.

Table 1

Results of comparative analysis of nonorthogonal configurations of inertial sensors

N	Type of configuration	Trace of correlation matrix of errors		
		without faults	2 faults	3 faults
1	5 sensors along the cone's generatrices	2.21	3.20	3.92
2	6 sensors along the cone's generatrices	1.79	2.13	4.50
3	4 sensors along the cone's generatrices and 1 along the symmetry axis	1.93	3.15	5.00
4	5 sensors along the cone's generatrices and 1 along the symmetry axis	1.70	2.18	3.35

Analysing information represented in Table 1 it is possible to make conclusion that the best variant is the fourth one. The mutual location of axes of the body reference frame O*xyz* is represented in Fig. 3.

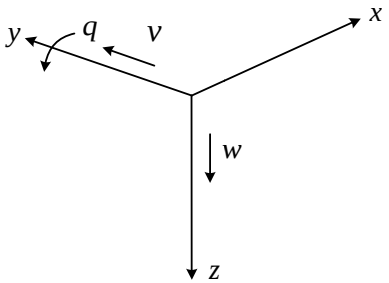

Fig. 3. O*xyz* is the body reference frame: O*z* is the vertical down-directed axis; O*x* is the longitudinal axis; O*y* is the lateral axis

Orientation of redundant measuring instrument consisting of 5 sensitive elements (SE) located on a cone's generatrices and 1 sensitive element located along the symmetry axis is shown in Fig. 4.

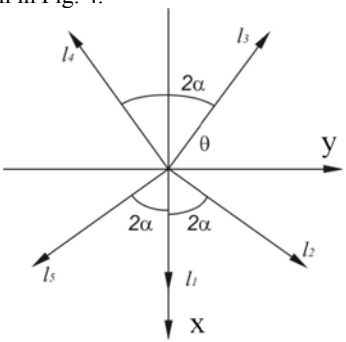

Fig. 4. Orientation of 5 SE on a cone's generatrices and 1 SE along the symmetry axis

The following notations are used in Fig. 4: *xyz* is the navigation reference frame; $l_1 l_2 l_3 l_4 l_5 l_6$ is the measuring reference frame; angles θ, α are defined in the following way: θ=54°44', α=36º.

Matrix of directional cosines for the above presented nonorthogonal configuration becomes

$$\mathbf{H} = \begin{bmatrix} \sin и & -\cos и & 0 \\ \cos 2б \sin и & -\cos и & \sin 2б \sin и \\ -\cos б \sin и & -\cos и & \sin б \sin и \\ -\cos б \sin и & -\cos и & -\sin б \sin и \\ \cos 2б \sin и & -\cos и & -\sin 2б \sin и \\ 0 & -1 & 0 \end{bmatrix}. \quad (1)$$

The connection between the primary information measured by sensors and navigation information about angular rate can be represented in the following form [4]

$$\mathbf{l} = \mathbf{H}\mathbf{ш}, \quad (2)$$

where $\begin{bmatrix} l_1 & l_2 & \dots & l_n \end{bmatrix}^{\mathrm{T}}$ is the vector of projections of the angular rate, measured in the measuring reference frame; $\begin{bmatrix} \omega_x & \omega_y & \omega_z \end{bmatrix}^{\mathrm{T}}$ is the vector of projections of the angular rate in the navigation reference frame; n is quantity of the inertial sensors in the measuring redundant instrument. The matrix $\mathbf{H}$ is called the matrix of transformation between navigation reference frame and redundant measuring frame.

Taking into consideration (2), the formula for angular rate determination can be represented in the following form [4]

$$\mathbf{ш} = \mathbf{H}^{-1}\mathbf{l}. \quad (3)$$

The expression for the pseudoinverse matrix based on the Moore-Penrose algorithm can be represented in the following form

$$\mathbf{H}^{-1} = (\mathbf{H}^T\mathbf{H})^{-1}\mathbf{H}^T = [\mathbf{H}_{\omega_x}^{-1}\ \mathbf{H}_{\omega_y}^{-1}\ \mathbf{H}_{\omega_z}^{-1}]. \quad (4)$$

Expressions (1) – (4) describe the aggregation algorithm for the measuring system represented in Fig. 1.

Mathematical model of plant

The above stated problem can be solved on the example of a small UAV assigned for observation of weather conditions including temperature, atmosphere pressure, humidity and wind above the ocean and remote terrains [6]. The linearized model of a plant can be represented by the set of equations in the state space

$$\begin{cases} \dot{\mathbf{x}} = \mathbf{A}\mathbf{x} + \mathbf{B}\mathbf{u} \\ \mathbf{y} = \mathbf{C}\mathbf{x} + \mathbf{D}\mathbf{u} \end{cases}. \quad (5)$$

Dynamic of the longitudinal motion of UAV can be described by the state vector [6, 7]

$$\mathbf{x} = [v, w, q, \theta, h, \Omega]^{\mathrm{T}},$$

where v, w are horizontal and vertical components of the true airspeed; q is the pitch angular rate; θ is an angle of the pitch; h is the flight altitude; Ω is an angular rate of the motor (in revolutions per minute). Control of the longitudinal motion is implemented by means of elevator deviations and control of engine thrust. So, the control vector looks like

$$u = [\delta_e, \delta_{th}]^{\mathrm{T}},$$

where δ_e, δ_{th} are deviations of elevator and steering wheel for traction control, respectively.

The output vector can be represented in the following form

$$\mathbf{y} = [V_a, \alpha, q, \theta, h],$$

where V_a is the true airspeed, α is an angle of the attack.

The linearized equations of the longitudinal motion can b described in the following way

$$\begin{cases} \dot{v} = Y_v v + Y_w w + Y_q q + Y_\theta \theta + Y_h h + Y_\Omega \Omega + Y_{\delta_e} \delta_e + Y_{\delta_{th}} \delta_{th}; \\ \dot{w} = Z_v v + Z_w w + Z_q q + Z_\theta \theta + Z_h h + Z_\Omega \Omega + Z_{\delta_e} \delta_e + Z_{\delta_{th}} \delta_{th}; \\ \dot{q} = M_v^y v + M_w^y w + M_q^y q + M_\theta^y \theta + M_h^y h + M_\Omega^y \Omega + M_{\delta_e}^y \delta_e + M_{\delta_{th}}^y \delta_{th}; \\ \dot{\theta} = H_{\omega_y}^{-1} q; \\ \dot{h} = \theta + H_v v + H_w w; \\ \dot{\Omega} = h + T_v v + T_w w + T_{\delta_{th}} \delta_{th}. \end{cases}$$

(6)

Taking into consideration the expression (6), matrices $\mathbf{A}$ and $\mathbf{B}$ of the state space model (5) can be represented in the following form

$$\mathbf{A} = \begin{bmatrix} Y_v & Y_w & Y_q & Y_\theta & Y_h & Y_\Omega \\ Z_v & Z_w & Z_q & Z_\theta & Z_h & Z_\Omega \\ M_v & M_w & M_q & M_\theta & M_h & M_\Omega \\ 0 & 0 & H_{\omega_y}^{-1} & 0 & 0 & 0 \\ H_v & H_w & 0 & 1 & 0 & 0 \\ T_v & T_w & 0 & 0 & 1 & 0 \end{bmatrix}, \quad \mathbf{B} = \begin{bmatrix} Y_{\delta_e} & Y_{\delta_{th}} \\ Z_{\delta_e} & Z_{\delta_{th}} \\ M_y & M_y \\ 0 & 0 \\ 0 & 0 \\ 0 & T_{\delta_{th}} \end{bmatrix}.$$

(7)

Elements of the matrix **A** in (7) are components depending on UAV aerodynamics and motor construction. The matrix **B** in (7) is used for implementation of two controls [8]. The above given matrices (7) are matrices of states **A** and observations **B**. Nowadays synthesis of robust control in many cases is based on the state space models (5). For the above mentioned UAV such matrices

can be obtained using AeroSim package of MatLab system [9]. So, matrices of state, control and observation in the numerical form look like

$$\mathbf{A}=\begin{bmatrix} -0.1956 & 0.7253 & -1.9446 & -9.7757 & -0.0001 & 0.0099 \\ -0.6170 & -3.6757 & 19.4157 & -0.9719 & 0.001 & 0 \\ 0.5233 & -3.7373 & -3.8346 & 0 & 0 & -0.0068 \\ 0 & 0 & 1.000 & 0 & 0 & 0 \\ 0.0989 & -0.9951 & 0 & 19.9998 & 0 & 0 \\ 26.2099 & 2.6058 & 0 & 0 & -0.0118 & -2.0073 \end{bmatrix};$$

$$\mathbf{B}=\begin{bmatrix} 0.2901 & 0 \\ -1.6556 & 0 \\ -20.9145 & 0 \\ 0 & 0 \\ 0 & 0 \\ 0 & 299.711 \end{bmatrix}; \quad \mathbf{C}=\begin{bmatrix} 0.9951 & 0.0989 & 0 & 0 & 0 & 0 \\ -0.0049 & 0.0498 & 0 & 0 & 0 & 0 \\ 0 & 0 & 1 & 0 & 0 & 0 \\ 0 & 0 & 0 & 1 & 0 & 0 \\ 0 & 0 & 0 & 0 & 1 & 0 \end{bmatrix}.$$

For the model of the lateral motion the vector of states becomes $\mathbf{x}=[v,\ p, r, \varphi, \psi]^T$, where β is the angle of slide; p, r are angular rates of roll and yaw, φ, ψ are angles of roll and yaw [10]. Vector of control is defined as $\mathbf{u}=[\delta_\alpha, \delta_r]^T$, where δ_a, δ_r are angles of deviations of ailerons and rudder. The vector of output looks like $y=[\beta,\ p, r, \varphi, \psi]^T$ [6, 7].

The linearized equations of the lateral motion can be written in the following form

$$\begin{cases} \dot{v}=X_v v+X_p p+X_r r+X_\varphi \varphi+X_{\delta_a}\delta_a+X_{\delta_r}\delta_r; \\ \dot{p}=M_v^x v+M_p^x p+M_r^x r+M_\varphi^x \varphi+M_{\delta_a}^x \delta_a+M_{\delta_r}^x \delta_r; \\ \dot{r}=M_v^z v+M_p^z p+M_r^z r+M_\varphi^z \varphi+M_{\delta_a}^z \delta_a+M_{\delta_r}^z \delta_r; \\ \dot{\varphi}=H_{\omega_x}^{-1} p; \\ \dot{\psi}=H_{\omega_z}^{-1} r. \end{cases} \tag{8}$$

Matrices of the aerodynamic coefficients $\mathbf{A}$ and $\mathbf{B}$ look like

$$\mathbf{A}=\begin{bmatrix} Y_v & Y_p & Y_r & Y_\varphi & Y_\psi \\ L_v & L_p & L_r & L_\varphi & L_\psi \\ N_v & N_p & N_r & N_\varphi & N_\psi \\ 0 & H_{\omega_x}^{-1} & 0 & 0 & 0 \\ 0 & 0 & H_{\omega_z}^{-1} & 0 & 0 \end{bmatrix}, \quad \mathbf{B}=\begin{bmatrix} X_{\delta_a} & Y_{\delta_r} \\ M_{\delta_a}^x & L_{\delta_r} \\ M_{\delta_a}^z & M_{\delta_r}^z \\ 0 & 0 \\ 0 & 0 \end{bmatrix}. \tag{9}$$

The matrix (9) obtained on expressions (8) in the generalized case can be used for two controls [8]. The expressions (6) – (9) were obtained taking into consideration the reference frame represented in Fig. 1. Such reference frames and notations correspond to foreign technical literature [7, 11]. Here Y means the first derivative of the lateral force by the appropriate parameters; L and N are moments by the roll and yaw. The numerical matrices of state, control and observation obtained by means of AeroSim Package look like

$$\mathbf{A}=\begin{bmatrix} -0.5702 & 1.9786 & -19.9017 & 9.7757 & 0 \\ -3.3984 & -16.7803 & 8.0757 & 0 & 0 \\ 0.5434 & -2.1680 & -0.8281 & 0 & 0 \\ 0 & 1 & 1 & 0.0994 & 0 \\ 0 & 0 & 0 & 1.0049 & 0 \end{bmatrix};\ \mathbf{B}=\begin{bmatrix} -0.9669 & 2.4680 \\ -77.6673 & 1.3287 \\ -3.0995 & -14.1149 \\ 0 & 0 \\ 0 & 0 \end{bmatrix};$$

$$\mathbf{C}=\begin{bmatrix} 0.05 & 0 & 0 & 0 & 0 \\ 0 & 1 & 0 & 0 & 0 \\ 0 & 0 & 1 & 0 & 0 \\ 0 & 0 & 0 & 1 & 0 \\ 0 & 0 & 0 & 0 & 1 \end{bmatrix}.$$

It should be noted that matrix $\mathbf{D}$ is zero matrix for both longitudinal and lateral motions.

Robust structural synthesis

H_∞-synthesis is one of methods using for design of the feedback control systems based on determination of the bounded frequency responses as functions of the singular numbers. There is an approach for robust systems design, when the sufficient condition of the robust stability is formulated in the form of norms, bounded by the weighting transfer functions. This approach is accepted in such automated computer-aided facilities for the robust systems optimal design as the Robust Control Toolbox [12].

The synthesized system consists of the plant and controller described by the matrix transfer functions $\mathbf{G}(s)$, $\mathbf{K}(s)$ respectively. These transfer functions must be fractionally-rational and proper. The generalized control object represents a system with two inputs and two outputs. The vector $\mathbf{w}$ represents the external output, which, in the general case, consists of disturbances, measurement noise and command signals. The input vector $\mathbf{u}$ represents the control signals. The output vector $\mathbf{z}$ determines the quality of the control processes. For example, it can be characterized by the command signal tracking error, which must be equal to zero in the ideal case. The output vector $\mathbf{y}$ represents the vector of the observed signals, which are used for feedback organization.

There are the different statements of the tasks, which can be solved by the method of mixed sensitivity. One of these problems can be described by the generalized system and the optimization criterion in the following form [12]

$$J(\mathbf{G},\mathbf{K}) = \left\| \begin{bmatrix} \mathbf{W}_1(\mathbf{I}+\mathbf{GK})^{-1} \\ \mathbf{W}_2\mathbf{K}(\mathbf{I}+\mathbf{GK})^{-1} \\ \mathbf{W}_3\mathbf{GK}(\mathbf{I}+\mathbf{GK})^{-1} \end{bmatrix} \right\|_\infty ,$$

here $\mathbf{W}_1, \mathbf{W}_2, \mathbf{W}_3$ are weighting transfer functions of the sensitivity functions [12].

$$\mathbf{K}_{\text{опт}} = \arg \inf_{\mathbf{K}_{\text{опт}} \in \mathbf{K}_{\text{доп}}} J(\mathbf{G},\mathbf{K}) . \tag{10}$$

In the problem (10) the necessity to limit an error of the command signal tracking, the control signal and the output signal respectively are taking into account. The structural chart, which explains the statement of this problem, is represented in Fig. 5.

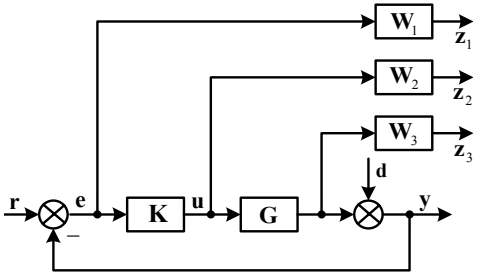

Fig.5. The structural chart for the method of mixed sensitivity with bounding of the error of the command signal tracking, the control signal and the output signal

The singular numbers of the closed transfer matrix functions from the command signal $\mathbf{r}$ to the signals of an error, input signals and output signal $\mathbf{e}$, $\mathbf{u}$, $\mathbf{y}$ [12] can be used for the quantitative estimation of the stability margins and frequency responses of the system.

Results of the synthesized system with the robust controller are represented in Figures 6.

Simulation results prove robust stability of the system in conditions of parametrical disturbances.

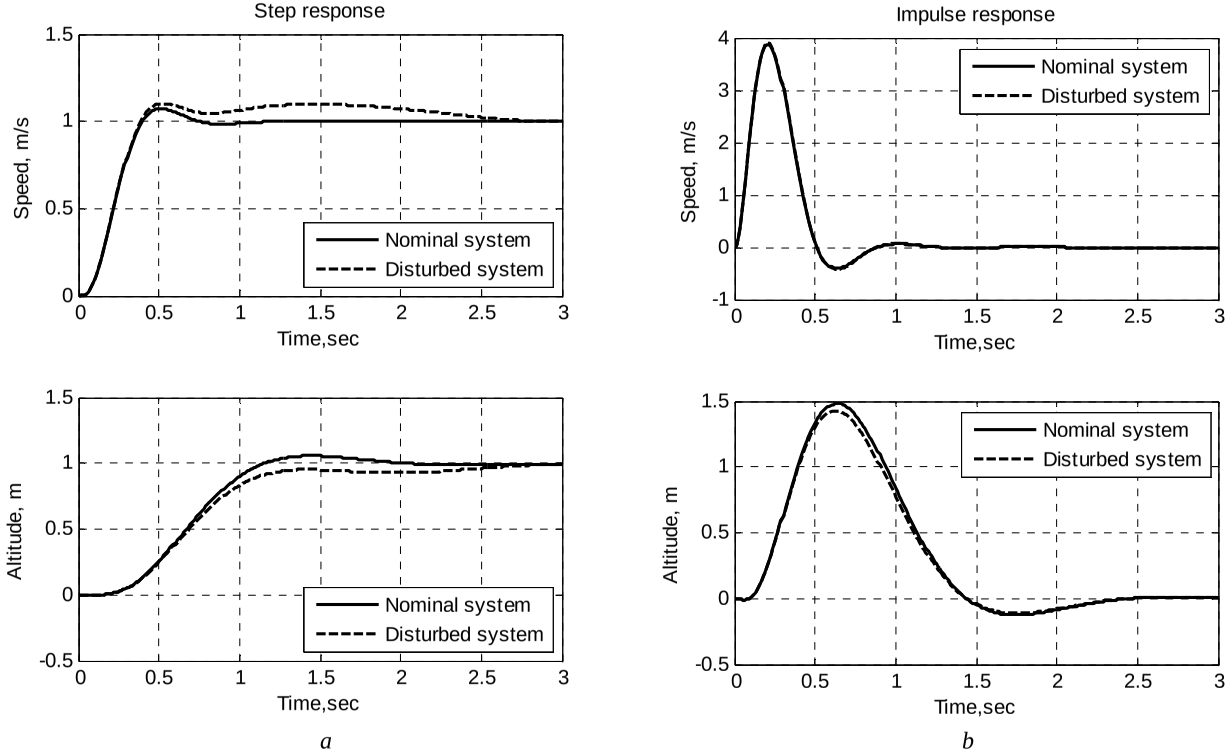

a *b*

Fig. 6. Results of robust controller synthesis of the system for the longitudinal (*a*) and lateral (*b*) motion

The aggregation algorithm for determination of navigation information entering from the redundant measuring instrument was obtained. The mathematical model of UAV longitudinal and lateral motions taking into consideration redundant measuring instrument based on inertial sensors has been done. The robust control system based on the robust structural synthesis, namely, H_∞ synthesis, was carried. Combination of navigation information redundancy and robust controller provides improvement of a system's functioning in difficult conditions of UAV real operation.

References

1. Cheng J., Dong J., Landry R.J., Chen D.A. Novel optimal configuration form redundant MEMS inertial sensors based on the orthogonal rotation method. *Sensors*, 2014, vol. 14(8), pp. 13661-13678.
2. Nilsson J.O., Skog I., Handel P. An open-source multi inertial measurement unit (MIMU) platform. Inertial Sensors and Systems
3. Sushchenko O. A., Bezkorovainyi Y. N., Novytska N. D. Nonorthogonal redundant configurations of inertial sensors, 2017 IEEE 4th International Conference Actual Problems of Unmanned Aerial Vehicles Developments (APUAVD).
4. Epifanov A. D. Redundant Systems of Aircraft Control. Moscow: Mashinostroenie, 1978. 178 p. (in Russian)
5. Sushchenko O. A., Bezkorovainyi Y. N., Novytska N. D. Theoretical and Experimental Assessments of Accuracy of Nonorthogonal MEMS Sensor Aarrays / EasternEuropean Journal of Enterprise Technologies , no. 3, pp. 78-87.
6. Holland G.J., Webster P.J., Curry J.A. et al. The aerosonde robotic aircraft: a new paradigm for environmental observations, Bulletin of the American meteorological society, vol. 82, no. 5, 2001, pp.889-901.
7. D. McLean. Automatic Flight Control Systems. Prentice Hall, Inc., 1990, 593 p.
8. Jeromel J.C., Peres P.L., Souza S.R. Convex Analysis of Output Feedback Control Problems: Robust Stability and Performance, IEEE Trans, on Automatic Control. -1996. - Jul. - Vol. 41, № 7. - P. 903-1003.
9. AeroSim – Aerospace Technology. Mode of direct access: AeroSimwww.aerospace-technology.com/contractors/training/aerosim/
10. Tunik A.A., Kim J.C., Yoo C.S. The Parameter Optimization of Aircraft's Control Law from the Viewpoint of Some Airworthiness Requirements // Proceedings of the 12th Korea Automatic Control Conf. "97 KACC". ICASE Publ. - Seoul. -1997. - P. 1651-1654.
11. Stevens Brian L. Aircraft Control and Simulation / Brian L. Stevens, Frank F., Lewis.– [2nd ed.]. – John Wiley & Sons Inc., 2003. – 665 p.
12. Skogestad S. Multivariable Feedback Control / Skogestad S., Postlethwaite I. – New York: Jonh Wiley, 1997. – 559 p.